High-temperature superconducting quantum interference device with cooled LC resonant circuit for measuring alternating magnetic fields with improved signal-to-noise ratio

Longqing Qiu, Yi Zhang, Hans-Joachim Krause, Alex I. Braginski, and Alexander Usoskin

Citation: Review of Scientific Instruments **78**, 054701 (2007);
View online: https://doi.org/10.1063/1.2735561
View Table of Contents: http://aip.scitation.org/toc/rsi/78/5
Published by the American Institute of Physics

Articles you may be interested in

High-sensitivity cooled coil system for nuclear magnetic resonance in kHz range
Review of Scientific Instruments **85**, 114708 (2014); 10.1063/1.4901964

Input Circuits for Pulsed NMR
Review of Scientific Instruments **37**, 268 (2004); 10.1063/1.1720155

High-temperature superconducting quantum interference device with cooled *LC* resonant circuit for measuring alternating magnetic fields with improved signal-to-noise ratio

Longqing Qiu
Institute of Bio- and Nanosystem (IBN-2), Research Center Juelich, D-52425 Juelich, Germany and Pohl Institute of Solid State Physics, Tongji University, Shanghai 200092, People's Republic of China

Yi Zhang, Hans-Joachim Krause, and Alex I. Braginski
Institute of Bio- and Nanosystem (IBN-2), Research Center Juelich, D-52425 Juelich, Germany

Alexander Usoskin
European High Temperature Superconductors GmbH & Co. KG, D-63450 Hanau, Germany

(Received 26 January 2007; accepted 21 March 2007; published online 2 May 2007)

Certain applications of superconducting quantum interference devices (SQUIDs) require a magnetic field measurement only in a very narrow frequency range. In order to selectively improve the alternating-current (ac) magnetic field sensitivity of a high-temperature superconductor SQUID for a distinct frequency, a single-coil *LC* resonant circuit has been used. Within the liquid nitrogen bath, the coil surrounds the SQUID and couples to it inductively. Copper coils with different numbers of windings were used to cover the frequency range from <1 to nearly 100 kHz. A superconducting coil made of $YBa_2Cu_3O_{7-\delta}$ tape conductor was also tested. With the *LC* circuit, the signal-to-noise ratio of measurements could be improved typically by one order of magnitude or more in a narrow frequency band around the resonance frequency exceeding a few kilohertz. The best attained equivalent magnetic field resolution was 2.5 fT/$\sqrt{\text{Hz}}$ at 88 kHz. The experimental findings are in good agreement with mathematical analysis of the circuit with copper coil. © *2007 American Institute of Physics.* [DOI: 10.1063/1.2735561]

I. INTRODUCTION

Certain applications of superconducting quantum interference devices (SQUIDs), such as eddy current nondestructive evaluation,[1] photoscanning,[2] measurement of susceptibility of magnetic beads,[3] and (low field) nuclear magnetic resonance,[4] may require high field sensitivity only at a distinct frequency.

A high-sensitivity low-T_c SQUID magnetometer usually involves a tightly coupled flux transformer, which consists of a pickup coil wound from niobium (Nb) wire and a planar input coil usually patterned from a thin Nb film. However, in the case of high-T_c devices, given the absence of a flexible, bondable high-T_c wire, only planar structures have been used to date.[5]

Low-temperature tuned SQUID amplifiers with resonating input circuit were analyzed in depth, both theoretically and experimentally, in the 1980s.[6] In the case of high-T_c SQUIDs, it has been shown that resonant transformers made of normal conducting wires could improve the sensitivity of SQUID magnetometers at frequencies ranging from several kilohertz to the order of 1 MHz. Yang and Enpuku introduced a capacitor connecting two copper coils of the transformer located in nitrogen bath. This resonant-type coupling circuit improved the magnetic field resolution to 26 fT/$\sqrt{\text{Hz}}$ at 6.37 kHz.[7] He *et al.* used a similar resonant-type coupling circuit and obtained $B_N=5.67$ fT/$\sqrt{\text{Hz}}$ at 954 kHz, even though the pickup coil was kept at room temperature.[8]

In this article we report on a new design of resonant-type coupling circuit suitable for high-T_c SQUID. Our *LC* circuit consists of only one coil, which acts as both a pickup coil and an input coil; the coil surrounds the high-temperature superconductor (HTS) SQUID within the liquid nitrogen bath and is shunted by a capacitor. Several copper wire coils with different numbers of turns were investigated with capacitors having appropriate capacitances in order to obtain a wide range of resonance frequencies. Additionally, one superconducting coil wound from $YBa_2Cu_3O_{7-\delta}$ (YBCO) tape conductor was also tested. These simple *LC* circuits improved the signal-to-noise ratio (SNR) of measurements more effectively than the ac flux transformers mentioned above. We attained field resolution below 4 fT/$\sqrt{\text{Hz}}$ even at a low frequency of only several kilohertz.

The radio frequency (rf) SQUID magnetometer used for this work is of the so-called substrate resonator type.[9] A YBCO thin film washer structure is patterned on the $SrTiO_3$ substrate with the dimensions of $10\times10\times1$ mm^3. This setup serves as a tank circuit (resonator) and as a flux concentrator. On the resonator substrate, a small rf washer SQUID with a square hole of 150 μm^2 is positioned in flip-chip geometry. This SQUID magnetometer achieved the field-to-flux transfer coefficient $\partial B/\partial\phi$ of 1.85 nT/Φ_0. White SQUID flux noise of about $20\mu\Phi_0/\sqrt{\text{Hz}}$ was measured, corresponding to a field resolution of about 40 fT/$\sqrt{\text{Hz}}$.

 © 2007 American Institute of Physics

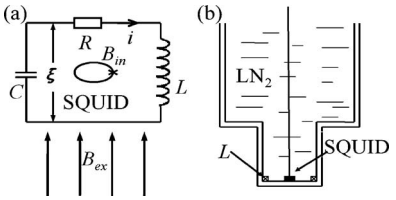

FIG. 1. The equivalent circuit (a) and the experimental arrangement (b) of the *LC*-circuit-assisted SQUID inside the liquid nitrogen bath.

II. PRINCIPLE AND CIRCUIT ANALYSIS

A. Signal gain

The equivalent circuit of the SQUID with the cooled *LC* circuit and the experimental arrangement in the cryostat are sketched in Figs. 1(a) and 1(b), respectively. The SQUID is located in the center of the copper coil of the *LC* circuit. Both the SQUID and the coil are situated in liquid nitrogen in a cryostat.

We assume an *LC* circuit with resonant angular frequency ω_0 is exposed to an external ac magnetic field $B_{\mathrm{ex}}=B_0\cos\omega t$. The flux $\Phi=N(\pi r^2)B_{\mathrm{ex}}$ through the coil loop induces an electric potential $\xi=-d\Phi/dt=\omega_0 N\pi r^2 B_0\sin\omega_0 t$ across the coil [see Fig. 1(a)], if $\omega=\omega_0$. The current flowing in the *LC* circuit can be written as

$$I_\omega 0=\frac{\xi}{R}=\frac{\omega_0 N\pi r^2 B_0\sin\omega_0 t}{R}=\frac{QN\pi r^2 B_0\sin\omega_0 t}{L}, \tag{1}$$

where $Q=\omega_0 L/R$ is the quality factor of the *LC* circuit, and L, R, N, and r are the inductance, resistance, number of turns, and mean radius of the coil, respectively. The induced current I_{ω_0} generates an additional field B_{add}. The total magnetic field B_{in} in the coil center [see Fig. 1(a)] is

$$\begin{aligned}B_{\mathrm{in}}&=B_{\mathrm{add}}+B_{\mathrm{ex}}=\frac{\mu_0 N I_{\omega_0}}{2r}+B_{\mathrm{ex}}=\frac{\mu_0 QN^2\pi r B_0\sin\omega_0 t}{2L}\\&\quad+B_0\cos\omega_0 t=\sqrt{\left(\frac{\mu_0 QN^2\pi r}{2L}\right)^2+1}\\&\quad\times B_0\sin(\cos\omega_0 t+\varphi),\end{aligned} \tag{2}$$

in which φ is the phase shift caused by the superposition of the two different signals, B_{add} and B_{ex}. Thus, the signal gain G_S can be expressed as

$$\begin{aligned}G_S&=\sqrt{\left(\frac{\mu_0 QN^2\pi r}{2L}\right)^2+1}\\&\approx\frac{\mu_0 QN^2\pi r}{2L}\quad(\text{when }\mu_0 QN^2\pi r/2L\gg 1).\end{aligned} \tag{3}$$

All parameters in formula (3) are either known or can be easily measured.

When the quality factor Q is expressed as $\omega_0 L/R$, and R as $N\times 2\pi r\times\rho_l$, where ρ_l denotes the resistance of copper wire per unit length, expression (3) then becomes

$$G_S=\frac{\mu_0\omega_0 N}{4\rho_l}\quad\text{or}\quad\frac{G_S}{N}=\frac{\mu_0\omega_0}{4\rho_l}. \tag{4}$$

This simple formula indicates that the signal gain G_S increases with increasing number of turns N and resonant frequency ω_0, once the diameter of the copper wire has been selected. Also, G_S is inversely proportional to ρ_l. Consequently, cooling a coil to 77 K results in a signal gain G_S which is 7.5 times higher than that at room temperature.

B. Noise gain

Unfortunately, the *LC* circuit contributes also an additional flux noise to the SQUID. Only if the signal gain G_S is larger than the noise gain G_N, the *LC* circuit improves the SNR of the measurement.

The noise of the system consists of two sources: the intrinsic noise of the SQUID and the Johnson noise of the *LC* circuit. In the relevant range of frequency f, the intrinsic noise of the SQUID is almost constant and amounts to approximately 40 fT/$\sqrt{\mathrm{Hz}}$ above 1 kHz. The noise equivalent magnetic field spectral density of an air-cored coil can be defined as[10]

$$\mathrm{Noise}_{LC}=S(f)\mathrm{TF}(f)\sqrt{4k_B TR_S}, \tag{5}$$

where the $S(f)=2/\pi^2 ND^2 f$ is the sensitivity of the coil, with $D=2r$; the transfer function $\mathrm{TF}(f)$ is given as

$$\mathrm{TF}(f)=\frac{1}{1-(f/f_0)^2+j\times 2\mathrm{DF}(f/f_0)}, \tag{6}$$

with the damping factor $\mathrm{DF}=(1/2)R\sqrt{C/L}$, and at the resonant frequency f_0, the amplitude of the transfer function $\mathrm{TF}(f)$ can be simplified as

$$|\mathrm{TF}(f_0)|=\frac{\sqrt{L/C}}{R}, \tag{7}$$

which is an expression for the quality factor (Q) of the resonator.

Thus we can obtain the noise equivalent magnetic field spectral density of the system,

$$\mathrm{Noise}_{\mathrm{Total}}=\sqrt{S_{\Phi-\mathrm{SQUID}}+S^2(f)Q^2\times 4k_B TR_S}. \tag{8}$$

Using the expression mentioned earlier, the noise gain G_N can be simplified as

$$\begin{aligned}G_N&=\sqrt{1+\frac{(2/\pi^2 ND^2 f_0)^2(2\pi Lf_0/2\pi rN\rho_l)^2(4k_B TR_S)}{S_{\Phi-\mathrm{SQUID}}}}\\&=\sqrt{1+\frac{64L^2 k_B T}{\pi^3 N^3 D^5\rho_l}}\approx 8\sqrt{\frac{L^2 k_B T}{\pi^3 N^3 D^5\rho_l}}\end{aligned} \tag{9}$$

The last approximation is valid when the noise of the *LC* circuit dominates the total noise density.

The signal-to-noise ratio improvement factor is the signal gain to noise gain ratio (SNGR). Combining formulas (4) and (9), the SNGR is

$$\mathrm{SNGR}=\frac{G_S}{G_N}=\frac{\mu_0\omega_0 N^2 D^2\pi\sqrt{\pi NDk_B T}}{32\rho_l Lk_B T}. \tag{10}$$

From this formula, it can be deduced that it is easier to get a high gain in the high frequency regime. Furthermore, the inductance of the coil is dependent on the number of turns, N, and the relationship is roughly $L\propto N^2$.[10]

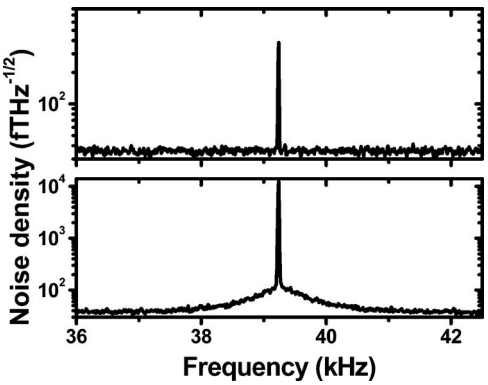

FIG. 2. Measured magnetic field noise density spectra without (top) and with (bottom) an *LC* circuit. Without the *LC* circuit, the signal and noise were 384 fT and 35 fT$\sqrt{\text{Hz}}$, respectively; with the *LC* circuit, the signal seen by the SQUID was 12.3 pT and noise was 108 fT$\sqrt{\text{Hz}}$.

Typically, for a coil of 50 mm in diameter wound with enameled copper wire of 0.12 mm diameter, and immersed in liquid nitrogen, the SNGR should be higher than 1 when $N>60$ at 10 kHz.

III. RESULTS

A. Experimental test of principle

In order to experimentally test the principle, an ac magnetic field having an amplitude of about 400 fT at $f=39.2$ kHz was applied to the SQUID with and without an *LC* circuit ($r=11.5$ mm, $N=800$, $C=0.015$ μF). Figure 2 shows the measured noise density spectra without (upper curve) and with (lower curve) the *LC* circuit. The spectra were recorded with a HP 3562A dynamic signal analyzer, 0–100 kHz. The frequency f of the magnetic excitation field was adjusted to the resonant frequency f_0 of the *LC* circuit. In this case, the signal gain G_S reached 32, while the noise gain G_N was 3.1 only. Thus we obtained SNGR of 10.3.

B. *LC* circuit with normal conductor coil

Coils with different numbers of turns were measured at a range of resonant frequencies to compare calculated and experimentally obtained signal and noise gains and to evaluate the highest attainable SNGR. All coils were wound on a PVC coil former using enameled copper wire of 0.12 mm diameter. The specific resistance ρ_l [see formula (4)] of this copper wire was measured to be 0.30 Ω/m at 77 K. The coil former had an outer diameter of 50 mm, an inner diameter of 40 mm, and a width of 11 mm. The number of turns was varied from 100 to 3600. For each coil, the shunt capacitance was varied from 0.33 μF to 47 pF in ten steps. The capacitor was placed either in liquid nitrogen or at room temperature. This had no effect on the results. Therefore, for convenience, the capacitors were usually placed at room temperature.

Due to the parasitic capacitance (C_p) between the coil windings, each coil has its own intrinsic resonant frequency $f_{\text{intr}}=(1/2)\pi\sqrt{LC_p}$, even without connecting to any capacitor. The f_{intr} sets the upper frequency limit for the coil. Physical parameters of the coils are listed in Table I. The measured quality factors (Q_M) were obtained by full-width-at-half-maximum method.

TABLE I. Ohmic resistance R in liquid nitrogen, inductance L, intrinsic resonance frequency f_{intr}, parasitic capacitance C_p, measured quality factor Q_M at f_{intr}, and theoretical quality factor $L\omega/R$ at f_{intr} of different coils.

N	R (Ω)	L (mH)	f_{intr} (kHz)	C_P (pH)	Q_M	$L\omega/R$
100	3.7	0.61	771	63.4	⋯	⋯
200	7.9	2.46	257	208	⋯	⋯
400	15.1	8.31	88.4	407	73.7	305
600	22.7	19.6	55.5	439	74	301
800	30.1	35.5	45.8	357	76.3	339
1000	37.7	56.1	36.4	360	80.9	340
1200	45.9	76.9	32.3	322	92.3	340
1800	70.0	175	24.4	246	97.6	383
2400	95.2	312	20.0	205	100	412
3000	121	487	17.1	179	114	432
3600	147	696	14.5	174	72.5	430

Table I shows roughly the expected scaling behavior: $N\propto\sqrt{L}\propto R\propto 1/f_{\text{intr}}$. Theoretical quality factors $L\omega/R$ are significantly larger than the measured quality factors Q_M at f_{intr}, because the parasitic capacitance losses were not considered.

Spectral noise measurements were performed at different resonance frequencies f_0 using the set of coils and capacitors described above. From the measured spectra (not shown here), we extracted the signal gain G_S data plotted in Fig. 3(a) and the noise gain G_N plotted in Fig. 3(b). Figure 3(c) shows the SNGR curves calculated from measured signal gain and noise gain at different resonant frequencies.

The signal gain G_S of all coils increases with the frequency until it reaches its maximum at f_{max}, which is located somewhere below f_{intr} corresponding to the last point of each curve (except for the $N=100$ coil). The signal gain G_S of all coils in Fig. 3(a) agrees very well with Eq. (3), taking the measured quality factor Q_M at different f_0. All curves of G_S normalized against N and G_S/N were stacked up together; they fitted well the expression $\mu_0\omega/4\rho_l$ [Eq. (4)], except in the frequency range near f_{intr} as seen in the inset of Fig. 3(a). The deviations of the measured G_S/N are due to the measured quality factor being lower than the theoretical value, $Q_M<L\omega/R$. This can be attributed to the losses of parasitic capacitance.

The noise gain increases with N and the first point of each curve agrees well with Eq. (9). According to this expression [Eq. (9)], G_N should be independent of frequency, but the measured G_N tends to decrease with increasing frequency. This is so because the measured quality factor Q_M is less than its theoretical value and the total noise in Eq. (8) decreases accordingly.

At any given frequency, both G_S and G_N increase with increasing N and the SNGR is the result of competition between G_S and G_N. As expected from Eq. (10), SNGR shown in the inset of Fig. 3(c) increases with the frequency, but is limited by the intrinsic frequency. The maximal experimental SNGR values were usually obtained close to the intrinsic frequencies of the coils. Values above 10 were obtained from several kilohertz on, but it is easier to get a high SNGR at higher frequencies. The best experimental SNGR of 16.3 was obtained at 88 kHz, corresponding to an equivalent magnetic

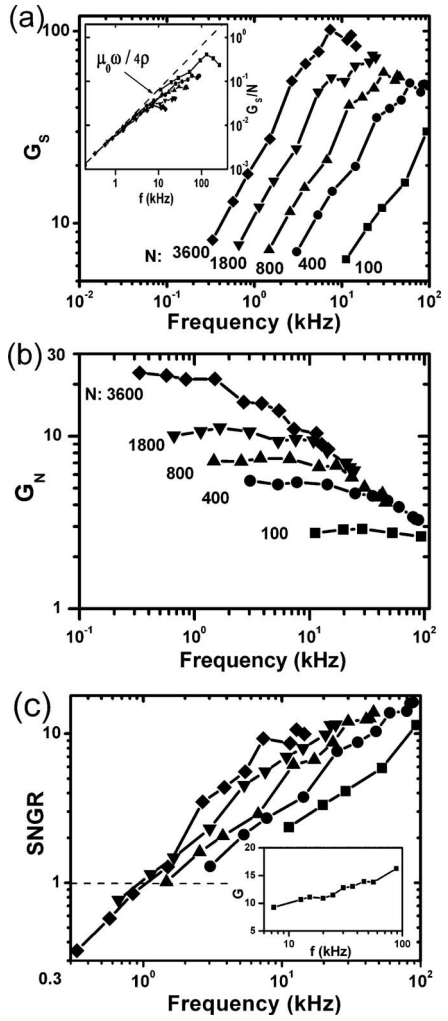

FIG. 3. Signal gain G_S (a), noise gain G_N (b), and SNGR (c) of different *LC* circuits. The inset in (a) shows the measured G_S/N vs ω compared to the plot of Eq. (4), and the inset in (c) displays the maximal SNGR obtained at different frequencies.

field resolution of 2.5 fT/$\sqrt{\text{Hz}}$. Figure 4 compares theoretical and measured maximum SNGR as a function of frequency. Theoretical values were calculated at intrinsic frequencies of coils, while the experimental best SNGR values were obtained slightly below f_{intr}.

Both the calculated and experimental SNGRs increased with frequency. At low frequency theoretical and measured

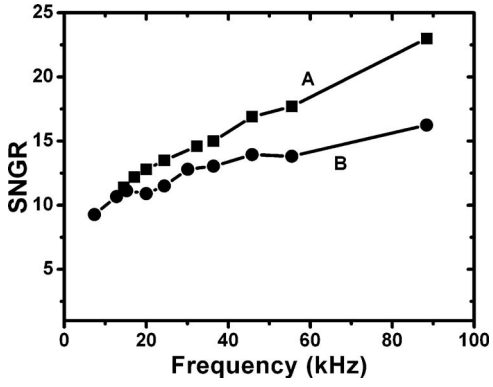

FIG. 4. The theoretical (A) and measured (B) maximal SNGR vs frequency.

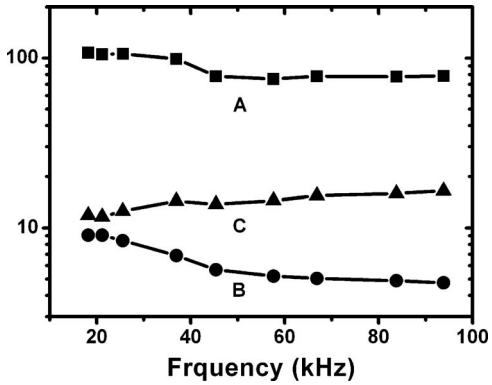

FIG. 5. Plots of signal gain (A), noise gain (B), and SNGR (C) vs frequency for the superconducting coil circuit.

values coincided while at about 90 kHz the experimental SNGR was 30% lower that the calculated. The slight difference between f_{intr} and the frequency of measurement could contribute to the discrepancy. Overall, calculation and experiment agreed reasonably well for the normal conducting coil circuit.

C. *LC* circuit with superconducting coil

We also tested one superconducting coil. The 49-turn coil was wound from a 4 mm wide tape of YBCO superconductor, deposited on 100 μm thick stainless steel substrate, with a 100 μm thick interlayer insulation tape.[11] Each end of the superconducting tape was soldered to a copper lead. This coil had a mean diameter of 36.7 mm and inductance of about 90 μH, nearly seven times lower than that of the normal coil with $N=100$. The measured parasitic capacitance of the coil was 3.94 pF, corresponding to an intrinsic frequency of above 8 MHz. The shunt capacitance was varied from 1 to 0.037 μF in nine steps. The capacitors were attached directly to coil's ends and immersed in liquid nitrogen to minimize the inductance of normal leads. Signal gains and thus SNGR values determined with capacitors in LN_2 were significantly higher than in the case of room-temperature capacitors (mounted outside of the cryostat). Clearly, at the very low coil inductance, the inductance and resistance of normal leads to a capacitor were not negligible. Using the same method as before, we measured the gains versus frequency (see Fig. 5).

In contrast to normal coil circuits, the G_S values measured between 16 and 90 kHz were relatively frequency independent but somewhat higher at lower frequencies. The model calculations are not applicable when the circuit losses are dominated by shunt capacitance and not the coil. The SNGR increase with frequency resulted from the corresponding G_N decrease.

To directly compare the SNGR of the superconducting and normal coil circuits, two additional normal coils were fabricated. One had the same turn number as the superconducting coil ($N=49$, $L=172$ μH) and the other the same inductance ($N=37$, $L=90$ μH). Figure 6 shows the SNGR of these three coil circuits. For comparison, the maximal SNGR curve of circuits with normal conducting coils is also plotted.

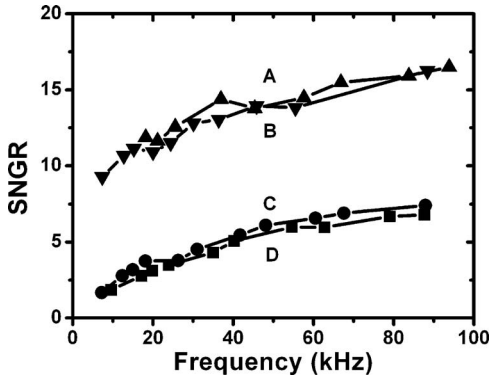

FIG. 6. SNGR of normal and superconducting coil circuits: (A) maximal SNGR of normal coils, (B) superconducting coil, (C) $N=49$ (normal), and (D) $N=37$ (normal).

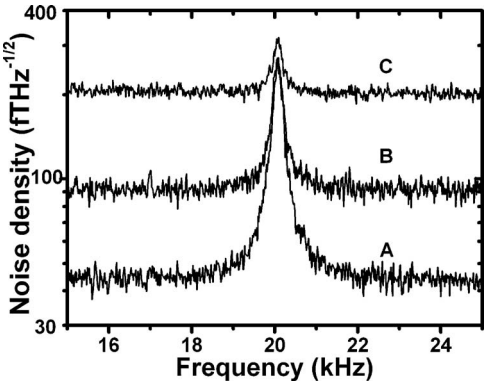

FIG. 7. Noise density and 20 kHz signal spectra for a resonant *LC* circuit at three different noise levels of the SQUID magnetometer

The maximum SNGRs obtained at different frequencies using a range of normal conducting coils and that of the superconducting coil are almost the same. The normal coils with the equivalent turn number or inductance resulted in a dramatically lower SNGR in the whole frequency range due to the coil Ohmic losses. Hence, the advantage of using a superconducting coil was clearly demonstrated.

D. Effect of SQUID noise

The SNR of measurements using a normal coil at resonance is usually determined by the *LC* circuit, because its noise at resonance is much higher than that of the SQUID itself. Figure 7 shows three noise spectra with superposed 20 kHz signal for the same *LC* circuit, but three different noise levels of the SQUID magnetometer: 45, 90, and 200 fT/$\sqrt{}$Hz. The working (operating) point of the same rf SQUID was adjusted to its optimum (spectrum A), somewhat away from the optimum (spectrum B), and strongly misadjusted (spectrum C). The SQUID noise made no significant contribution to the signal peak of 270 fT as long as the SQUID noise level was below 100 fT/$\sqrt{}$Hz (spectra A and B). Only in the case of spectrum C, when the *LC* circuit and the SQUID had comparable noise levels, signal peak increased to about 320 fT. Hence, introduction of the *LC* circuit significantly relaxes the requirements for SQUID noise level.

IV. DISCUSSION

We analyzed and experimentally evaluated a simple but effective *LC* resonant input circuit, which can remarkably improve the SNR of high-T_c SQUID ac field measurements at a distinct frequency. The analysis and experimental results agreed rather well for normal wire coils. The SNR of the ac magnetic field measurement was improved by typically one order of magnitude or more in the frequency range from several kilohertz to 100 kHz. The best magnetic field resolution of 2.5 fT/$\sqrt{}$Hz was obtained at 88 kHz. Requirements on SQUID noise can be relaxed, because the noise of the resonant *LC* circuit dominates the system noise.

Test of one very low inductance superconducting tape coil resulted in SNR improvement equivalent to that attained with a whole set of normal coils having much higher inductances. Higher inductance of the superconducting coil should result in higher SNR, but at the expense of bandwidth. The current tape conductor technology may permit significantly increasing the number of coil turns and inductance via thinner tape substrate and thinner interlayer insulation.

[1] H.-J. Krause and G. Donaldson, in *The SQUID Handbook, Fundamentals and Technology of SQUIDs and SQUID Systems*, edited by J. Clarke and A. I. Braginski (Wiley-VCH, Weinheim, 2006), Vol. II, pp. 453–459.
[2] J. Beyer, D. Drung, and T. Schurig, IEEE Trans. Appl. Supercond. **11**, 1162 (2001).
[3] T. Q. Yang, M. Abe, K. Horiguchi, and K. Enpuku, Physica C **412–414**, 1496 (2004).
[4] H. C. Seton, D. M. Bussell, J. M. S. Hutchison, and D. J. Lurie, IEEE Trans. Appl. Supercond. **5**, 3218 (1995).
[5] R. Cantor and D. Koelle, in *The SQUID Handbook, Fundamentals and Technology of SQUIDs and SQUID Systems*, edited by J. Clarke and A. I. Braginski (Wiley-VCH, Weinheim, 2004), Vol. I, p. 191.
[6] J. Clarke, A. T. Lee, M. Mück, and P. L. Richards, in *The SQUID Handbook, Fundamentals and Technology of SQUIDs and SQUID Systems*, edited by J. Clarke and A. I. Braginski, (Wiley-VCH, Weinheim, 2006), Vol. II, pp. 6–16.
[7] T. Q. Yang and K. Enpuku, Physica C **392–396**, 1396 (2003).
[8] D. F. He, H. Itozaki, and M. Tachiki, Supercond. Sci. Technol. **18**, S1 (2005).
[9] Y. Zhang, J. Schubert, and N. Wolters, Physica C **372–376**, 282 (2002).
[10] G. Dehmel, in *Sensors*, Magnetic Sensors Vol. 5, edsited by W. Göpel, J. Hesse, and J. N. Zemel (VCH, Weinheim, 1989), pp. 209–239.
[11] The conductor and coil were fabricated by European High Temperature Superconductors GmbH & Co. KG (EHTS).